

Language-Native Materials Processing Design by Text-First Database and Reasoning Large Language Model

Yuze Liu,^{1,3} Zhaoyuan Zhang,^{1,3} Xiangsheng Zeng,² Yihe Zhang,² Leping Yu,² Liu Yang,⁴ Lejia Wang,^{2, 5*} Xi Yu^{1*}

1. School of Science, Tianjin University, Tianjin 300072, China
2. Boron Matrix Advanced Materials Technology, No 3938 Wenchuan Road, Baoshan District, Shanghai City, 200949, China
3. Tianjin Language Intelligence Technology Co., Ltd., Haihe Education Park, Jinnan District, Tianjin City, 300350, China
4. College of Intelligence and Computing, Tianjin University, Tianjin 300072, China
5. School of Materials and Chemical Engineering, Ningbo University of Technology, Ningbo, 315211, China

* Authors to whom correspondence should be addressed: xi.yu@tju.edu.cn or wanglejia@nbut.edu.cn

Abstract: The preparation procedures of materials are often embedded narratively in experimental protocols, research articles, patents, laboratory notes, and are structured around procedural sequences, causal relationships, and conditional logic. The synthesis of boron nitride nanosheet (BNNS) polymer composites exemplifies this linguistically encoded decision-making systems, where the practical experiments involves interdependent multistage and path-dependent processes—exfoliation, functionalization, dispersion etc—each governed by heterogeneous parameters and contextual contingencies, challenging conventional numerical optimization paradigm for experiment design. We reformulate this challenge into a text-reasoning problem by a framework centered on text-first, lightly structured materials database, and large language models (LLMs) as text reasoning engines. We constructed a database captures evidence-linked narrative excerpts from the literature while normalizing only the minimum necessary entities, attributes, and relations to enable composite retrieval that unifies semantic matching, lexical cues, and explicit value filters. Building on this language-native, provenance-preserving foundation, the LLM operates in two complementary modes: retrieval-augmented generation (RAG), grounding outputs in retrieved evidence modules from the database, and experience-augmented reasoning (EAR), which leverages iteratively trained text guides derived from multi-source literature-derived narrative data as external references to inform reasoning and

decision-making. Rather than returning point-optimal settings, the system synthesizes interpretable, expert-style guidance—hypotheses, parameter windows, and citation-backed SOPs supporting iterative planning and failure diagnosis consistent with real laboratory practice. Applying this integration-and-reasoning framework, we demonstrate rapid, laboratory-scale optimization of BNNS preparation, highlighting how language-native data combined with LLM-based reasoning can significantly accelerate practical material preparation.

Introduction

Over the past decade, machine learning approaches in materials science have made significant strides in numeric and table-centric domains^{1,2,3,4}, where data adhere to stable schemas, as seen in ecosystems like the Materials Genome Initiative, crystallographic databases, and reaction repositories^{5,6,7}. However, a substantial portion of process-centric research and development (R&D) in materials science remains inherently language-native: experimental procedures^{8,9,10}, contingencies, and troubleshooting insights are predominantly documented in prose, where the nuances of order, conditionality, and provenance encode critical decision-making signals that extend beyond mere optimization to encompass practical decision making. Attempting to distill such narrative evidence into rigid tabular formats inevitably erodes these essential cues, rendering conventional supervised machine learning pipelines ill-equipped to harness the richest reservoirs of practical knowledge.

Boron nitride nanosheet (BNNS) based thermal conductive materials serve as a compelling exemplar of this challenge¹¹. As a pivotal material for thermal management in electronics and energy systems, the synthesis of these materials involves highly interdependent, multistage processes that are path-dependent and exhibit strong coupling across phases¹². Exfoliation, functionalization, dispersion and alignment of the BNNS et al are interwoven with conditional decision points, while parameters vary across disparate scales—from ultrasonic duty cycles and shear rates to surfactant chemistries and cure schedules. Upstream variables, such as pretreatments, reagent histories, and impurity profiles, propagate through interfaces and microstructures, profoundly influencing downstream processing windows. These procedures is fundamentally a decision-making task, where success depends on interpreting and applying stepwise instructions, heuristics, and failure diagnoses described in textual protocols, literature, and lab notes. In addition, real-world constraints—such as the cost of surfactants, time required for multi-step synthesis, availability of sonication or curing equipment, and tolerance to impurities—must be balanced alongside performance metrics like thermal conductivity. As a result, BNNS preparation poses a multifactorial, language-native decision problem, which conventional numeric- or

schema-based machine learning models struggle to address. Instead, what's required is a system that can interpret, reason over, and integrate textual procedural knowledge in a manner akin to human experts.¹³

Large language models (LLMs) offer a way to operate directly over such language-native evidence¹⁴, demonstrating their prowess in processing and synthesizing textual data at scale^{15,16,17,35}. This capability has led to numerous applications in chemistry and materials science¹⁸, enabling information extraction^{19,20,21,22}, literature-grounded QA^{23,24}, and agent systems^{25,26,27,28,29,30,31,33,34}. Particularly, the chain(tree)-of-thought reasoning intrinsic to advanced LLMs naturally encapsulates conditional logic, path branching, and other dynamic procedural elements embedded within natural language descriptions, positioning them as powerful text reasoning engines. This emergent capability allows models to mirror expert-like deliberation over narrative-driven processes, harmonizing with curated language-native representations i.e. in-context learning, to enable reasoning and decision-making in balancing real-world trade-offs. Similar context-plus-LLM reasoning paradigms have been explored in medicine for basic diagnostics and treatment decision-making, where models synthesize patient narratives and evidence to support clinical workflows³². However, current LLM driven agent systems in chemistry and materials treat natural language primarily as an intermediary bridging user query with structured tools or numerical models^{23,26,30}. Synthesis and preparation planning remains limited to relatively fixed chemical protocols, inferring reagent transformations without fully exploring the integration of reasoning models with textual data. Knowledge graphs^{36,37,38}, while adept at surfacing entities and relations for constraint-aware queries with provenance, impose high construction and maintenance costs at literature scale and flatten procedural nuances—such as dynamic conditional chains or feedback-driven semantic logic tied to practical trade-offs—into rigid triple-based abstractions, limiting their ability to support holistic decision-making in complex synthesis tasks.^{39,40,41,42}

In this study, we introduce a language–data integration-and-reasoning framework tailored for composite materials development that elevates natural-language evidence as a first-class data source. As shown in Figure 1, at its core we construct a heterogeneous, literature-grounded database by processing >3,500 BNNS–polymer composite papers with modular LLM prompts (see the Preparation module example in Fig. 3a). Full-article content—preparation protocols, characterization results, mechanistic inferences, theoretical modeling, and tabular data—is converted into lightly structured records. Each record comprises evidence-linked modules (actions, materials, instruments, conditions, conditional guards, characterization protocols, theoretical models, and mechanistic reasoning) co-stored with typed fields (e.g.,

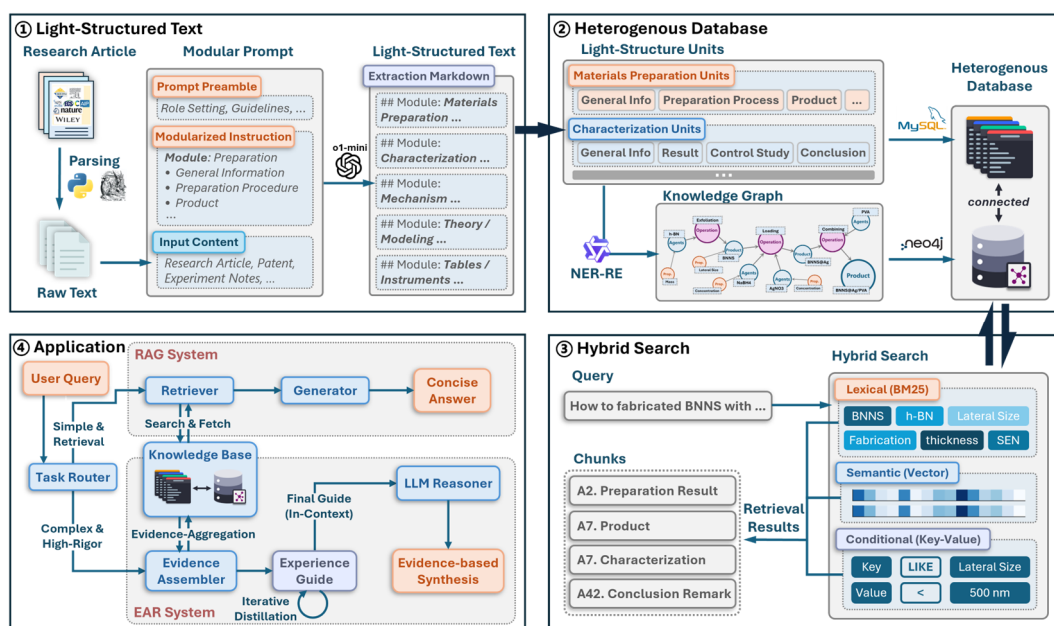


Figure 1: Framework of an intelligent AI system driven by a heterogeneous database for BNNS-based thermal conductive materials. (a) Light-structured text with hierarchical topic organization is generated from scientific literature using modular prompting to reconstruct information from unstructured texts. (b) The structured text is decomposed into semantic units, which are then converted into knowledge graphs via named entity recognition and relation extraction (NER-RE), forming a heterogeneous knowledge base. (c) Target text blocks are retrieved through hybrid methods including BM25, dense vector search, and numerical condition filtering. (d) The database is integrated into downstream AI systems such as retrieval-augmented generation (RAG) and structured data extraction pipelines, serving as a domain-specific knowledge repository and retrieval engine.

numeric ranges, categorical terms, textual qualifiers) and bidirectional provenance links to the source. The light structuring predefines a hard spine while preserving rich narratives under higher-level headings (e.g., preparation, characterization, mechanisms, modeling) and retaining verifiable, evidence-linked snippets at subheading level. This design improves categorization and reduces redundancy versus raw text—mitigating RAG issues such as chunk-level redundancy, fragmentation, and incoherence—while avoiding the data loss and extraction hallucinations observed with overly rigid schemas. Retrieval is multifaceted, operating along semantic (via dense embeddings), lexical (via keyword/BM25 matching), and relational (via value filters, such as lateral size < 500 nm or solvent = NMP) axes to honor meaning, precise terminology, and explicit constraints in unison. These data structures power a reasoning LLM operating in dual modes: Retrieval-Augmented Generation (RAG) for synthesizing literature-grounded insights with traceable citations, and Experience-Augmented Reasoning (EAR), which leverages iteratively trained text guides derived from the database of multi-source literature excerpts as external references, incorporating curated heuristics, failure modes, and laboratory priors as modular "experience units" to inform reasoning and decision-making. By addressing

path dependencies and practical trade-offs (e.g., cost, complexity, time, equipment constraints), this approach reframes BNNS preparation as a language-mediated decision-making task, surpassing schema-constrained, numeric optimization.

We applied this framework to accelerate laboratory-scale fabrication of customized BNNS under intricate, multistep protocols. Our results reveal that text-native data, coupled with LLM-driven reasoning, enables AI-assisted route selection and predictive troubleshooting unattainable through numeric, table-centric methods alone, paving the way for scalable, knowledge-intensive materials innovation.

Narrative and Lightly Structured Dataset

The dataset for BNNS–polymer thermally conductive composites was obtained by processing over 3,500 literature articles using the modular LLM prompts. The prompt was carefully designed and tuned to adopt the lightly structured narrative data (example used for the Preparation module was shown in Figure 3a). It predefined the hard structure and encompassed detailed narratives on heading 1 and 2, including preparation, characterization, theoretical modeling, mechanism study, and tabular data. The evidence-linked snippets was stored in the heading 3 and sub-heading preserved for verifiability. This light-structuring is central to our method. On one hand, compared to raw text, it improves content categorization and reduces redundant descriptions, providing more valuable, concise information for subsequent LLM processing and mitigated issues in traditional RAG systems such as information redundancy, fragmentation, and incoherence from chunking^{46,47,48,49}. This benefit is further evidenced in the RAG performance evaluations below. On the other hand, these modules preserve textual richness while imposing light constraints for parsability, enabling the preservation of experimental contexts and mechanistic reasoning as described in the introduction. We did attempt stricter schemas in the data extraction, but they led to data loss or fabrication due to the mismatch between the predefined schema and the flexible description in the literature paper. Thus, light-structuring balances fidelity and organization, preserving comprehensive narratives data, with evidence-linked snippets for verifiability.

Figure 2 (b)-(e) present the performance and structural analysis of this extraction process. Panels (b) show precision and recall scores for numerical information mapped from 80 sample articles to light-structured texts, generated by various LLMs using modularized prompting. The o1-mini and o3-mini models achieve the best overall results, with o3-mini reaching the highest recall (~0.85) and o1-mini offering strong balanced performance. While gemini-2 exhibits high recall, it suffers from hallucinations and reduced precision. Overall, we found reasoning models (e.g., o1-mini, o3-mini) significantly outperformed non-reasoning models (e.g., gpt-4o-mini, gpt-

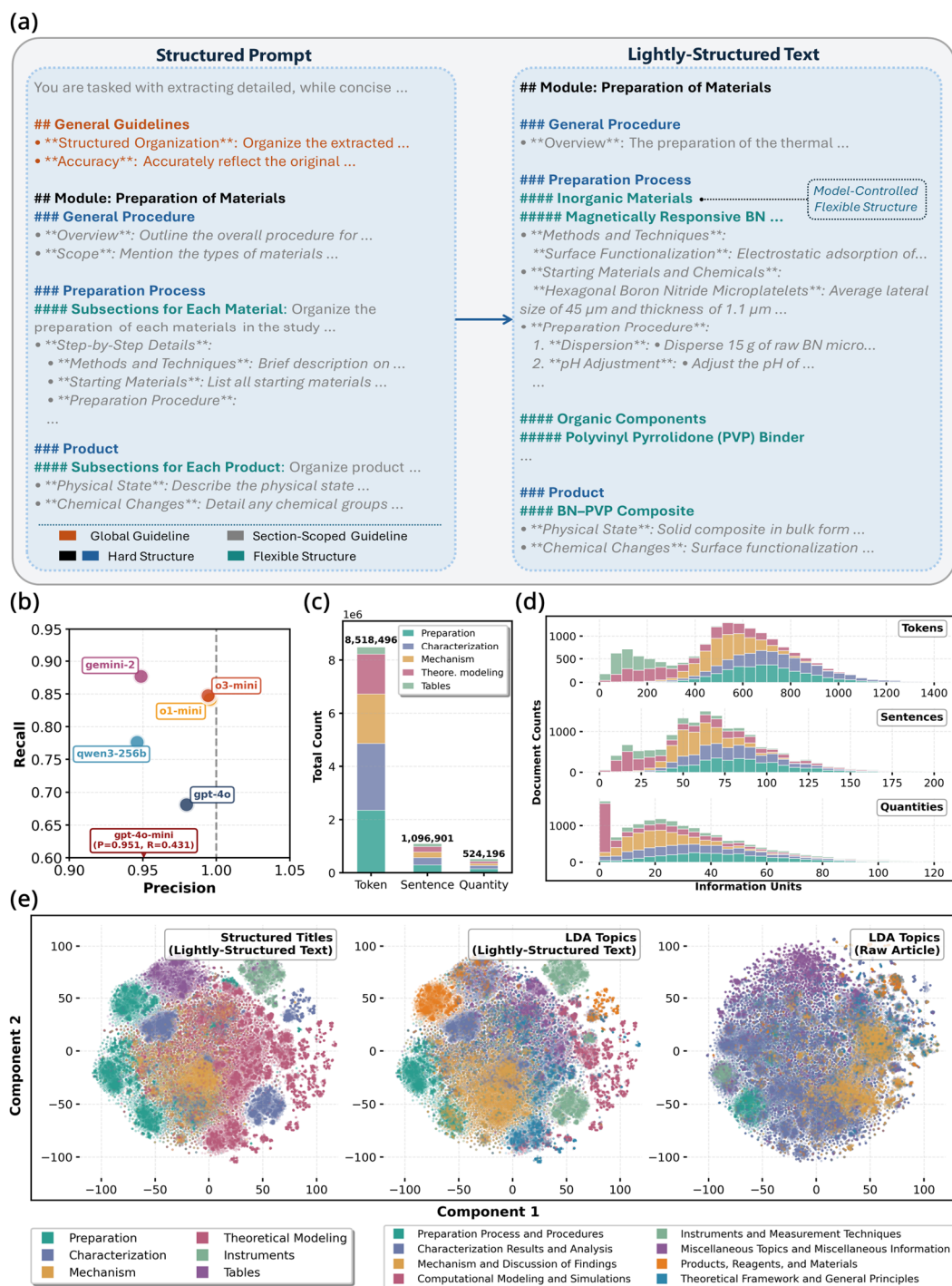


Figure 2: Extraction and analysis of light-structured texts. (a) Illustrates the construction of structured prompts by integrating hard and flexible structural headings, guided by domain-specific knowledge, to enable LLMs to generate lightly-structured text. (b) Shows the performance of different large language models in precision and recall when mapping numerical information from 80 sample articles (c-d) Distribution of information units in the extracted light-structured texts, with (d) illustrating the variation in token, sentence and quantity counts across documents. (e) t-SNE visualization of the light-structured text, comparing customized title (left 1) with LDA-derived topic (left 2); the strong alignment between title boundaries and topic distributions indicates that the light-structured title capture coherent semantic module, whereas LDA of original texts (right 1) reveals more topic mixing, highlighting the enhanced focus achieved through reconstruction.

4o), indicating their superior ability to understand relationships between described content and adhere to the lightly structured data formats specified in prompts. Panel (c) overviews the database's scale, segmented by content categories, with totals of 8,518,496 tokens, 1,096,901 sentences, and 524,196 quantities. Panel (d) illustrates long-tail distributions in tokens, sentences, and quantities across documents, where most entries are concise (e.g., under 250 tokens or 50 sentences), but a subset contains extensive details, reflecting literature variability; preparation and characterization dominate volume due to procedural and experimental content, while theoretical modeling part yields fewer but denser entries. Panel (e) provides t-SNE visualizations: semi-structured titles (left 1) show coherent semantic modules; LDA-derived topics in semi-structured articles (left 2) form tighter clusters compared to raw articles (right 1), indicating reduced topic mixing and enhanced focus through reconstruction. This structural improvement, evidenced by clearer cluster separation, aligns with light-structuring's advantages over raw text and underscores its necessity for BNNS–polymer processes, which involve diverse methods like mechanical exfoliation, liquid-phase sonication, CVD, electrospinning, and melt-extrusion, making rigid tables impractical.

Heterogeneous Database Schema

Figure 3a provides a granular view of the heterogeneous database schema, illustrating how lightly structured narrative datasets from raw articles are transformed into structured modules, and external indexes for efficient search.

Article metadata—including unique IDs, titles, abstracts, authors, and journals—is first extracted to anchor provenance. The "lightly-structured" layer organizes content into modular units linked by article IDs, capturing domain-specific narratives such as Preparation (with subfields like General, Process, Product, Conclusion), Characterization (Results, Instrument), Mechanism, Modeling (Theory, Methods, Simulation), and Tables.

The "Structure" layer further refines this into computable formats: Named Entity Recognition (NER) data extracts entities with attributes like type, name, value, and unit; Knowledge Graph (KG)^{37,38,40} nodes represent numbered elements with types, content, and values; and KG edges define relations (e.g., source-target links with types). This feeds into conditional search capabilities, allowing queries with keyword filters (e.g., thickness < 100 nm, time 0.5 h, speed = 500 rpm) to traverse relations and retrieve precise, evidence-linked results.

For scalable retrieval, external indexes are built from modules: a Vector Database stores module IDs with dense embeddings (using BGE-M3 models and FAISS L2

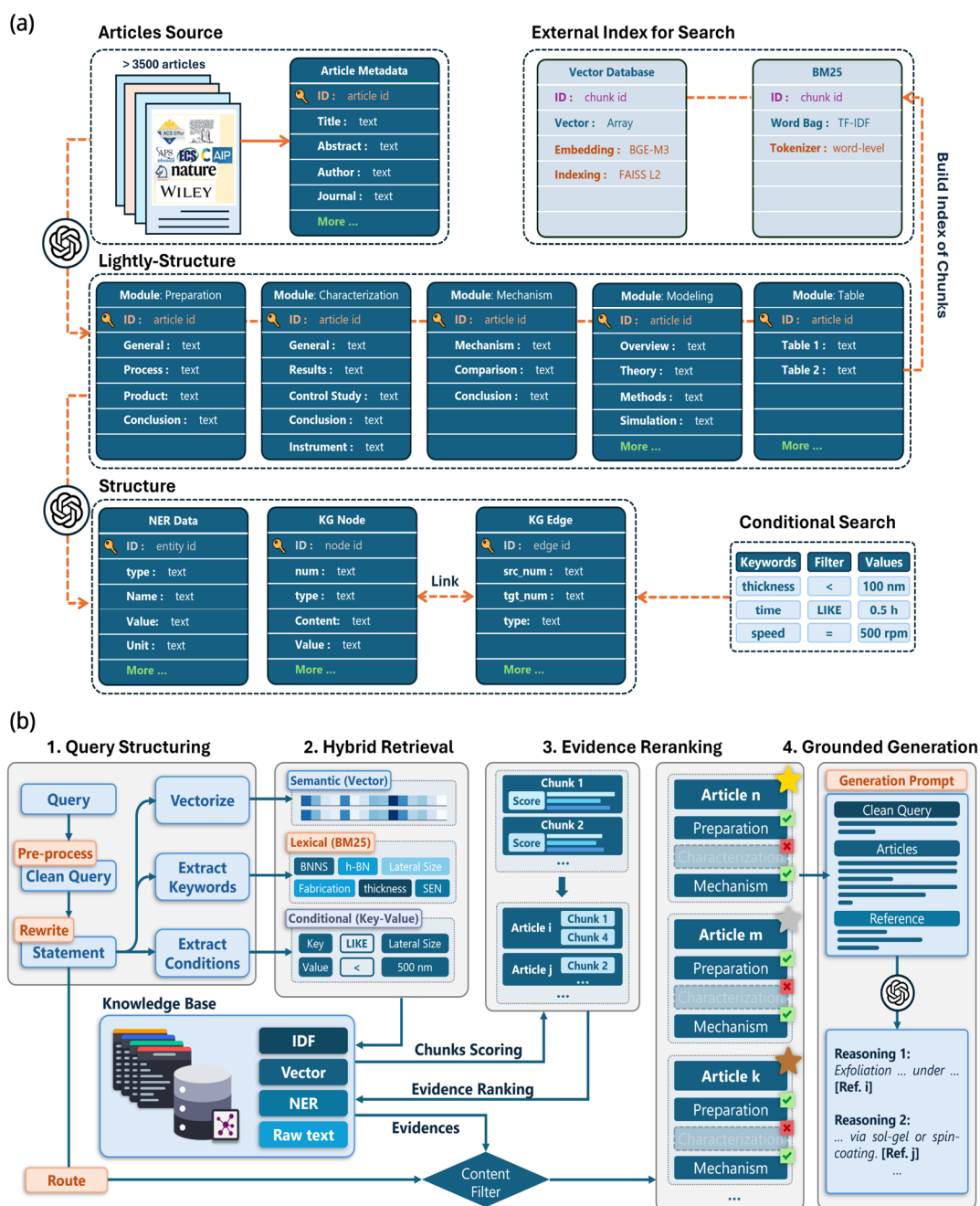


Figure 3: Schematic illustration of the heterogeneous database schema and the RAG architecture. (a) The heterogeneous database comprises three layers for each source article: (i) article content and associated metadata, (ii) lightly structured data in the form of language-native text, and (iii) structured data including name entities and knowledge graph. Multiple indices (BM25, vector, conditions) are built over these layers to support hybrid retrieval. (b) The RAG system built upon this database comprises four sequential stages: query structuring (where an LLM interprets and refines the user query to extract keywords and conditions), hybrid retrieval (combining dense, sparse, and conditional search to fetch relevant passages), evidence re-ranking (applying relevance scoring and content filtering to prioritize high-quality results), and grounded generation (where retrieved evidence is formatted into a reasoning-aware prompt to guide factually consistent LLM output).

weights and word-level tokenization for lexical matching. These indexes underpin the hybrid search mechanism, combining vector-based semantics, BM25 precision, and KG constraints to handle complex queries efficiently^{43,44,45}.

This schema enhances the database's interoperability, allowing seamless integration of numerical aggregations (e.g., from NER values) with narrative synthesis. This modular organization not only enables efficient indexing but also reduces redundancy in extracted narratives, as validated in subsequent analyses.

Composite Retrieval and RAG Pipeline

Figure 3b illustrates the end-to-end composite retrieval and RAG pipeline built on the heterogeneous database, enabling context-aware querying and generation for BNNS–polymer composites. Unlike traditional RAG systems that fragment articles into numerous disjoint chunks, leading to information fragmentation, retrieval failures, and hallucinations in LLM outputs, our approach leverages the lightly structured database to maintain coherent, compressed representations of article content^{50,51,52,53}. This organization—capturing modular sections like Preparation, Characterization, and Mechanism—allows selective retrieval of relevant modules based on query specifics, ensuring narrative completeness while remaining concise and focused.

Starting from a user query, the system performs query structuring by cleaning, rewriting statements, vectorizing and extracting keywords (e.g., BNNS, thickness, fabrication) and conditional constraints (e.g., key-value filters like lateral size < 500 nm). These elements drive multi-axis retrieval across the database layers: IDF for lexical relevance (BM25), vector embeddings for semantic matching, and NER for numerical filtering.

Retrieved modules undergo scoring and ranking, followed by a content filter to select relevant modules (e.g., Preparation, Characterization, Mechanism from articles). Only high-relevance modules proceed, preserving the integrity of empirical narratives without unnecessary dilution. The curated article evidence comprising references is assembled into a reasoning-aware generation prompt, along with the clean query, to drive LLM-based reasoning steps, producing verifiable outputs like multi-step SOPs, addressing challenges such as interfacial thermal resistance in BNNS–polymer interfaces.

Retrieval Effectiveness

The foundation of our system's efficacy lies in its composite retrieval mechanism. As shown in Figure 4(a), we evaluated hit rates on a set of 200 domain-specific queries (e.g., targeting specific BNNS dimensions or thermal enhancement mechanisms). Our framework achieves a first-hit success rate of 56.4%, significantly outperforming the

baseline RAG's 33.3%, and total top 12 hit increase from 56.4% to 84.6%. Failed hits decreased from 38.5% to 5.1%, indicating robust coverage. Figure 4(b) plots substantive match hit counts (relevant chunks with high semantic and lexical overlap) as a function of the top N retrieved results. Our hybrid search (combining 0.6 semantic + 0.3 BM25 + 0.1 KG weights) consistently yields the highest counts, surpassing vector-only and BM25 baselines by up to 40% at N=100. This demonstrates the framework's ability to scale retrieval depth while maintaining relevance, directly supporting the integration of text, relations, and numbers for multi-faceted reasoning in composites research.

Response Quality in RAG and Agentic Applications

Building on superior retrieval, the lightly structured data substrate empowers LLMs to generate accurate, quantifiable responses that mimic expert analysis, complete with citations and calculations.

To validate the framework's versatility, we enlisted human experts in BNNS-polymer composite materials studies to curate 60 representative queries, spanning five

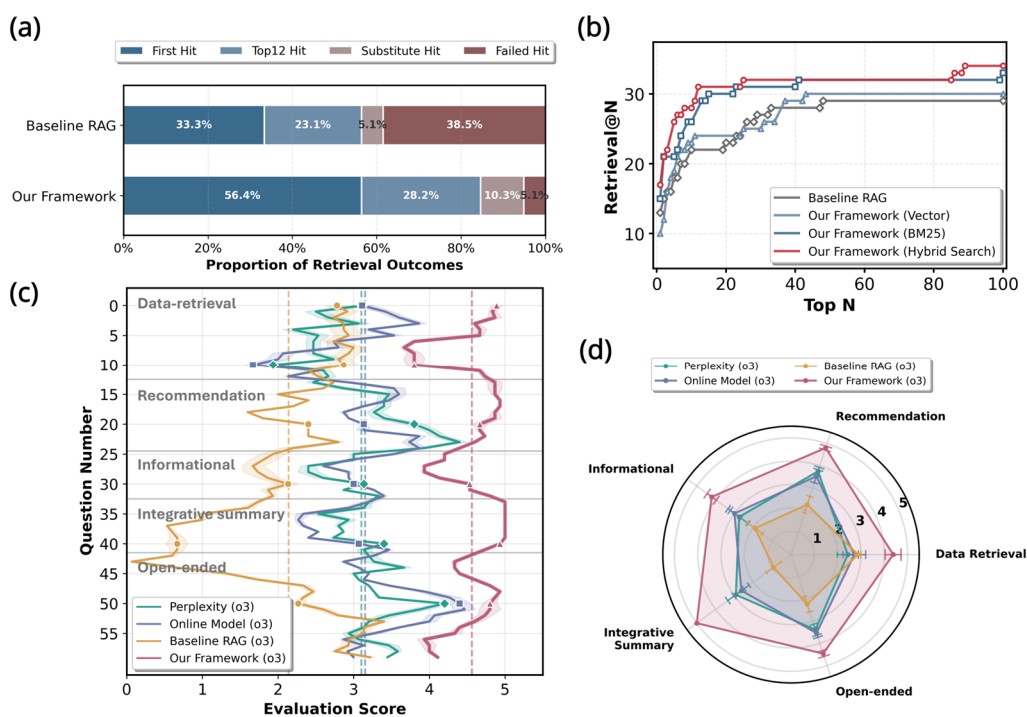


Figure 4: Evaluation of retrieval-augmented generation (RAG) performance. (a) Retrieval effectiveness comparison between the baseline RAG system and our proposed framework. (b) Comparison of Retrieval@N across four retrieval strategies: our hybrid framework, keyword-only retrieval, vector-only retrieval, and the baseline RAG system. (c-d) Expert-based manual assessment of 60 domain-specific questions in the BNNS-polymer composites domain, evaluating the factual accuracy and practical utility of generated responses. Methods compared include Perplexity (green), ChatGPT Online (blue), baseline RAG (yellow), and our framework (red), all using O3 as the agentic LLM.

categories: data-retrieval (e.g., extracting specific measurements), recommendation (e.g., suggesting preparation protocols), informational (e.g., explaining mechanisms), integrative summary (e.g., synthesizing trends across studies), and open-ended (e.g., hypothesizing novel composites). Detailed queries and ground-truth answers are provided in Supplementary Information (SI). Expert evaluators scored responses on a 1–5 scale for accuracy, completeness, and relevance, comparing our RAG system against: (1) Perplexity (GPT-o3 model) with web search capabilities; (2) an online model (o3, akin to ChatGPT with external access); and (3) an regular RAG model (Chunk Retrieval with GPT-o3 model).

Figure 4(c) visualizes scores by question number and type, revealing our framework's consistent superiority, with average scores exceeding 4.0 across categories—particularly in integrative summaries and recommendations, where multi-hop retrieval shines. Figure 4(d), a radar chart, summarizes this holistic outperformance, with our system achieving balanced high marks (4–5) on all axes, compared to baselines' uneven profiles. Overall, these results affirm the framework's role in reconciling language-native knowledge with computable elements, empowering verifiable guidance that mirrors expert practice and accelerates innovation in empirical sciences like composites research.

Comprehensive Benchmarking Across Query Types

To concretize the performance patterns illustrated in Fig. 4(c–d), we present three representative cases that span the spectrum of query complexity—from factual retrieval to expert-level reasoning—as detailed in Fig. 5. These cases illustrate how the organization of language-native knowledge critically shapes response quality. For brevity, we compare our framework against Perplexity (o3, web-enabled) and a baseline RAG system that employs conventional chunk-based document segmentation; all other components (retriever, generator, prompt template) are held constant. Full query-response pairs and additional examples across all five categories are provided in the Supplementary Information.

Case 1 (Data Retrieval): The user requests a precise thermal conductivity value under specific experimental conditions. Our system retrieves the relevant study, correctly identifies the matching data point, and performs a simple arithmetic operation to yield an accurate answer. In contrast, Perplexity fails to locate the pertinent source and instead combines values from two unrelated papers, producing a factually incorrect result. The baseline RAG retrieves the correct document but extracts an erroneous numerical value due to fragmentation: the target measurement is split across multiple chunks, disrupting contextual coherence and leading to misinterpretation.

Case 1: Precise Retrieval of Research Article Data

Query: For an electrospun PVA composite film with a BNNS-to-MWCNT mass ratio of 9:1, how much greater is its thermal conductivity than that of a pure BNNS/PVA film?

Our System (o3)

You asked: "(...the user queried question...)"

Main Content
From Article #2 [TARGET REFERENCE] (...)

Sample	Mass ratio (BNNS:MWCNT)	In-plane thermal conductivity λ / ($\text{W m}^{-1} \text{K}^{-1}$)
BNNS/PVA (pure BNNS filler)	10 : 0	9.536
BNNS-MWCNT/PVA	9 : 1	11.49

Absolute increase $\Delta\lambda = 11.49 - 9.536 \approx 1.95 \text{ W m}^{-1} \text{K}^{-1}$
Relative (percentage) increase $(11.49 / 9.536 - 1) \times 100 \% \approx 20.5 \%$

Conclusion
(...) an absolute gain of about $2 \text{ W m}^{-1} \text{K}^{-1}$, corresponding to roughly a 20 % enhancement. (...)

Accurate information acquisition and computation

Perplexity (o3)

(...) that uses a BNNS-to-MWCNT mass ratio of 9 : 1 is about $35.4 \text{ W m}^{-1} \text{K}^{-1}$. [REFERENCE]
(...) only BNNSs (no MWCNT bridge) at a comparable 90 wt % BNNS content is $\approx 70.4 \text{ W m}^{-1} \text{K}^{-1}$. [REFERENCE]
 $\Delta\text{TC} = 35.4 \text{ W m}^{-1} \text{K}^{-1} - 70.4 \text{ W m}^{-1} \text{K}^{-1} = -35.0 \text{ W m}^{-1} \text{K}^{-1}$
Relative change = -49.7%

Counterfactual Results

RAG-Chunk (o3)

- BNNS-only reference (...) ("BNNSPVA-III" in [REFERENCE]): (...)
- BNNS-MWCNT (...) mass ratio of 9:1 [TARGET REFERENCE]: (...)

Relative gain (percentage): $(28.7 / 18.63 - 1) \times 100 \% = 53 \%$ (...)

Incorrect value extracted from article

Case 2: Recommendation of Experimental Parameters

Query: In the DFT Calculations with Siesta, what is the mesh cutoff value used for the Real-Space Grid?

Our System (o3)

Because "mesh-cutoff" is not a universal constant but a user-defined parameter that is tightened or relaxed according to the size of the basis set, the density of valence electrons and the level of accuracy needed, different SIESTA studies adopt different values. (...)

Main Content

Study (system)	Purpose of the calculation	Mesh cut-off chosen	Rationale stated/implicit
Moraes et al. 2012 (...)	Band-structure tuning	150 Ry ($\approx 2040 \text{ eV}$)	"sufficient for accurate real-space grid integration"

(...)

How to choose an appropriate mesh-cutoff in SIESTA
1. Convergence target: decide an acceptable change in total energy/force (e.g. $\leq 1 \text{ meV/atom}$, $\leq 0.01 \text{ eV \AA}^{-1}$).
2. Start from a moderate value ($\approx 150 \text{ Ry}$ for s-p systems) and increase until energy, stress and forces stabilize.
(...)

Conclusion
(...) In the supplied literature the real-space grid cut-off spans from 150 Ry to 800 Ry (and even $\sim 300 \text{ Ry}$ in eV units) depending on the accuracy demanded by the property of interest. (...)

Reasoning Chain: Query constraints \rightarrow Evidence gathering \rightarrow Rule induction \rightarrow Conclusion

Perplexity (o3)

In the Siesta input file the real-space grid is fixed through the keyword:
"MeshCutoff 100 Ry"
Thus the requested mesh-cutoff (i.e., the energy equivalent that determines the grid density) is 100 Rydberg; when the run starts Siesta converts this into the closest FFT-friendly value and reports:
"InitMesh: Mesh cutoff (required, used) = 100.000 101.039 Ry"
so the grid actually employed is $\approx 101 \text{ Ry}$. [SIESTA-DOCS]

RAG-Chunk (o3)

(...)
The SIESTA calculations were carried out with a real-space grid "mesh-cutoff" (energy mesh) of 225 Ry [REFERENCE]

Both with erroneous query understanding

Case 3: Comprehensive Information Acquisition

Query: What is the prerequisite for achieving 'dual-alignment' using a dynamic magnetic field in the 3D printing process?

Our System (o3)

Here "dual-alignment" refers to the sequential combination of (...). The technique is best illustrated by Chen et al. ("Sequential Dual Alignments...", Adv. Mater., 2024) who used a rotating magnetic field (RMF) after extrusion to obtain highly planar mhBN platelets. [TARGET REFERENCE]

Main Content

1. Conceptual background
Dual-alignment works only if two alignment steps can act on the "same" population of fillers without interfering with, or canceling, each other: (...)

2. Practical prerequisites
The requirements fall into four inter-locking categories:
| Category | Prerequisite | Why it is needed | Typical ranges / remarks |
<... table content ...>

3. Common failure modes if prerequisites are not met
| Failure symptom | Likely missing prerequisite | Corrective action |
<... table content ...>

4. Parameter guideline (from Chen et al. unless noted)
- mhBN particle: $10 \mu\text{m} \times 0.3 \mu\text{m}$, Fe_3O_4 0.2 vol %. (...)

5. Cross-validation from related studies
• Itaoka et al. demonstrated that without magnetic coating, fields $>10 \text{ T}$ are required—highlighting why Fe_3O_4 functionalization is essential for practical RMF dual-alignment. [REFERENCE 7]
(...)

Conclusion
To realize dual-alignment during 3-D printing with a dynamic magnetic field you need: (...)

Reasoning Chain: Query constraints \rightarrow Theory analysis \rightarrow Counterfactual reasoning \rightarrow Comparison \rightarrow Conclusion

Perplexity (o3)

Achieving "dual-alignment" (i.e., being able to re-orient anisotropic fillers in two orthogonal directions during a single print run) requires that the suspended particles can rotate fast enough to follow the time-varying field. The prerequisite is therefore that the ink's viscosity be low enough that magnetic torque dominates viscous drag so the particles reach the imposed orientation within the short time (sub-second) available between extrusion and solidification [REFERENCE]

Not enough evidence supported

RAG-Chunk (o3)

The method relies on applying a time-varying (dynamic) magnetic field several times during the fabrication of a single layer. (...)
(...) every slice of the CAD model has to be "pre-segmented" into zones that share the same target orientation of the magnetically functionalised fillers.
In other words, the prerequisite for obtaining the so-called dual-alignment (different orientations in different parts of the same layer and between successive layers) is:
"First, elements within each print layer must be separated into groups according to their desired orientation." [REFERENCE]

Incorrect Mechanism: The mechanism shown is multi-directional orientation, not dual-alignment

Figure 5. Question-answering performance of a language-native heterogeneous knowledge base across three tasks of increasing complexity: (i) a factual query, (ii) multi-step reasoning with rule induction, and (iii) counterfactual analysis of failure modes. Baselines—perplexity-based retrieval and web-augmented ChatGPT—suffer from misinterpretation, incorrect citations, factual hallucinations, and shallow reasoning. In contrast, our system accurately retrieves relevant literature, extracts precise evidence, and demonstrates advanced scientific reasoning, including induction (Case 2) and structured counterfactuals (Case 3).

space grid calculations in interfacial thermal modeling—a parameter requiring contextual understanding of system scale and computational trade-offs. Our system synthesizes multiple literature examples, categorizes them by material system, and infers general design principles to justify its recommendation. Both Perplexity and the baseline RAG, however, default to replicating the parameter from a single highly ranked paper without adaptation or rationale, offering a non-transferable and thus non-actionable suggestion.

Case 3 (Mechanistic Reasoning): The user asks for an explanation of the “dual-alignment” mechanism and its prerequisite conditions. Our framework identifies the seminal paper on dual-alignment alongside supporting studies, reconstructs the authors’ causal reasoning, and extends the analysis by hypothesizing failure modes under violated assumptions—effectively simulating experimental pre-validation. The baseline RAG, by contrast, conflates this concept with “multi-directional orientation” from a 3D printing context, misattributing the underlying physics and delivering a conceptually incoherent summary.

These cases underscore a key insight: when all pipeline components except knowledge organization are controlled, the lightly-structured representation of language-native knowledge—where each module preserves the original narrative arc from general context to technical detail to conclusion—enables faithful retention of authorial logic and multi-hop inference. In contrast, chunk-based evidence, though retrievable, is inherently fragmented and short-range, often severing the very reasoning chains that domain experts rely on. This structural fidelity is what empowers our system to deliver not just accurate facts, but verifiable, expert-aligned guidance across the full range of BNNS fields inquiry.

Experience-Enhanced Iterative Design of SOP for BNNS

Extending the framework’s capabilities beyond RAG, we demonstrate its potential for iterative, experience-guided optimization in experimental design, leveraging the heterogeneous database to integrate empirical narratives. This addresses the trial-and-error nature of materials research by enabling LLMs to refine protocols dynamically, drawing on preserved linguistic descriptions of mechanisms and prior outcomes^{30,52,53,54,55,56,57}. In a concrete example, retrieval from the database yields lightly structured data from over 200 articles on BNNS preparation by ball milling, which undergoes iterative experience updates to composite a comprehensive guide that serves as an external reference for LLMs, aiding in the design of materials preparation processes. Figure 6 presents the experience-enhanced system architecture and a practical application to BNNS ball milling for BNNS fillers in polymer composites (see SI for detailed information). As illustrated in Figure 6(a), the system begins with a user

objective (e.g., "BNNS ball milling—parameters, process, characterization"), which queries the heterogeneous database via retrievers. Retrieved modules from articles are fed into an iterative loop: an E (experience) template initializes with summarization and distillation, followed by prompt-guided evolution, batch chunk integration, and optional human-in-the-loop quality reviews including entity comparison and hallucination checks. This refines the experience base through revisions, culminating in a final enhanced context that informs LLM inference for outputs like comprehensive guides. Unlike traditional RAG methods that handle fragmented chunks, this approach synthesizes vast literature into a logically coherent and content-rich guide (see supplementary information for the full text of the guide), fully described in natural language for human readability and modifiability—ideal for human-in-the-loop research.

Figure 6(b) showcases a case study applying this to iterative ball milling design for BNNS preparation, where supplying the resulting BNNS ball milling guide as an external reference to an LLM (using GPT-o3pro) enables the generation of detailed experimental conditions and standard operating procedures (SOPs). In this typical BNNS preparation example—prioritizing thin nanosheets (with minimal constraints on lateral size and a preference for hydroxyl or amino surface groups)—the LLM's expert recommendations, grounded in the generated guide, facilitated satisfactory exfoliation in just three rounds of experiments while resolving key defects.

In Trial 1, the LLM proposed a two-step scheme: pre-milling in a low-viscosity IPA/H₂O medium containing poly(vinylpyrrolidone) (PVP, $M_w \approx 35$ kDa) as a process control agent (PCA) with ZrO₂ media operated in on/off mode, followed by high-energy milling with urea as PCA, and post-centrifugation to collect the pellet. The IPA/H₂O–PVP system promotes shear-assisted liquid-phase exfoliation because PVP adsorbs on BN surfaces, providing steric and viscous damping that limits restacking and mitigates high-energy impacts. Subsequent milling with urea in minimal water is a plausible mechanochemical route to couple further thinning with surface functionalization, as urea can intercalate and form hydrogen-bonded adducts that increase surface polarity and dispersibility. However, the outcome (thickness ≈ 200 nm; lateral size ≈ 1.5 μ m; residual PVP; bead fracture) indicates that the chosen bead sizes (10 and 2 mm) and low viscosity placed the system in an impact-dominated regime, where normal forces dissipated energy as collisions rather than interlayer shear, yielding poor exfoliation. Post hoc urea treatment improves surface chemistry but cannot remediate a shear-limited mechanical stage.

Guided by this diagnosis, Trial 2 explicitly shifted variables to amplify shear: viscosity was increased by using H₂O with urea as PCA, PVP was relegated to a minor dispersant role, a smaller mixed bead ensemble (ZrO₂ beads of 5, 2, and 1 mm in a

5:3:2 ratio) was adopted, the ball to material ratio (BMR) was raised to $\approx 100:1$, and milling was run at 500 rpm without a separate functionalization step. Higher BMR typically increases collision frequency and total energy per mass of h BN, promoting interlayer slippage, while a denser, finer media bed homogenizes stresses and favors sustained micro shear events that, aided by stabilizers, keep freshly exposed surfaces apart. This protocol reduced the thickness of BN nanosheets (BNNS) to ≈ 50 nm but left PVP residues and aggravated bead wear. Impact contributions remained excessive under the combined high BMR and speed, and the single high-speed (10,000 rpm) pelleting step likely biased collection toward thicker flakes; the turbid supernatant implying loss of thinner fractions. Beyond an optimum, very high BMR shifts the process toward excessive impact, causing lateral fragmentation, defect formation, media contamination, and heat buildup. BMR therefore should be tuned to maximize shear-driven exfoliation while minimizing over-grinding.

Trial 3 further redirected the process toward shear dominance by using only smaller beads (2 and 1 mm, 1:1), moderating BMR to $\approx 80:1$ at 500 rpm, and removing PVP entirely. A urea–water mixture served as a single, viscous, paste like PCA that efficiently transmits shear and avoids polymer carryover. A two-window centrifugation was used for fractionation (2,000 rpm to pellet thick material, then 10,000 rpm to recover thin BNNS from the supernatant). This protocol yielded ≈ 40 nm BNNS with no polymer residue and no bead fracture, evidencing a deliberate transition from an impact-dominated to a shear-dominated exfoliation pathway through coordinated tuning of viscosity, bead size distribution, BMR, and centrifugation.

The LLM correctly identified the essence of this experiment as “viscous-protection exfoliation coupled with concurrent urea-enabled functionalization”. Rather than copying recipes, it reframed optimization from maximizing collisions to maximizing effective shear events, operationalized as a urea-thickened medium with tuned BMR and bead distribution to enhance delamination while enabling functionalization. It also treated experimentation as hypothesis-driven validation rather than a guarantee of specific outcomes, and iteratively refined parameters in response to feedback.

The system deliberately avoided sucrose and other hard-to-remove additives that, despite potential exfoliation benefits, cause foaming during milling and prolong dialysis, limiting scalability. This mechanism-centered approach contrasts with aggregator-style recommendations that mix heterogeneous protocols (e.g., NaOH pretreatment, multiple polymers, inconsistent post-processing) and often lack coherence.

Across the three trials, the LLM-guided protocol sequence achieved an $\approx 80\%$ thickness reduction while eliminating polymer-residue-related post-processing,

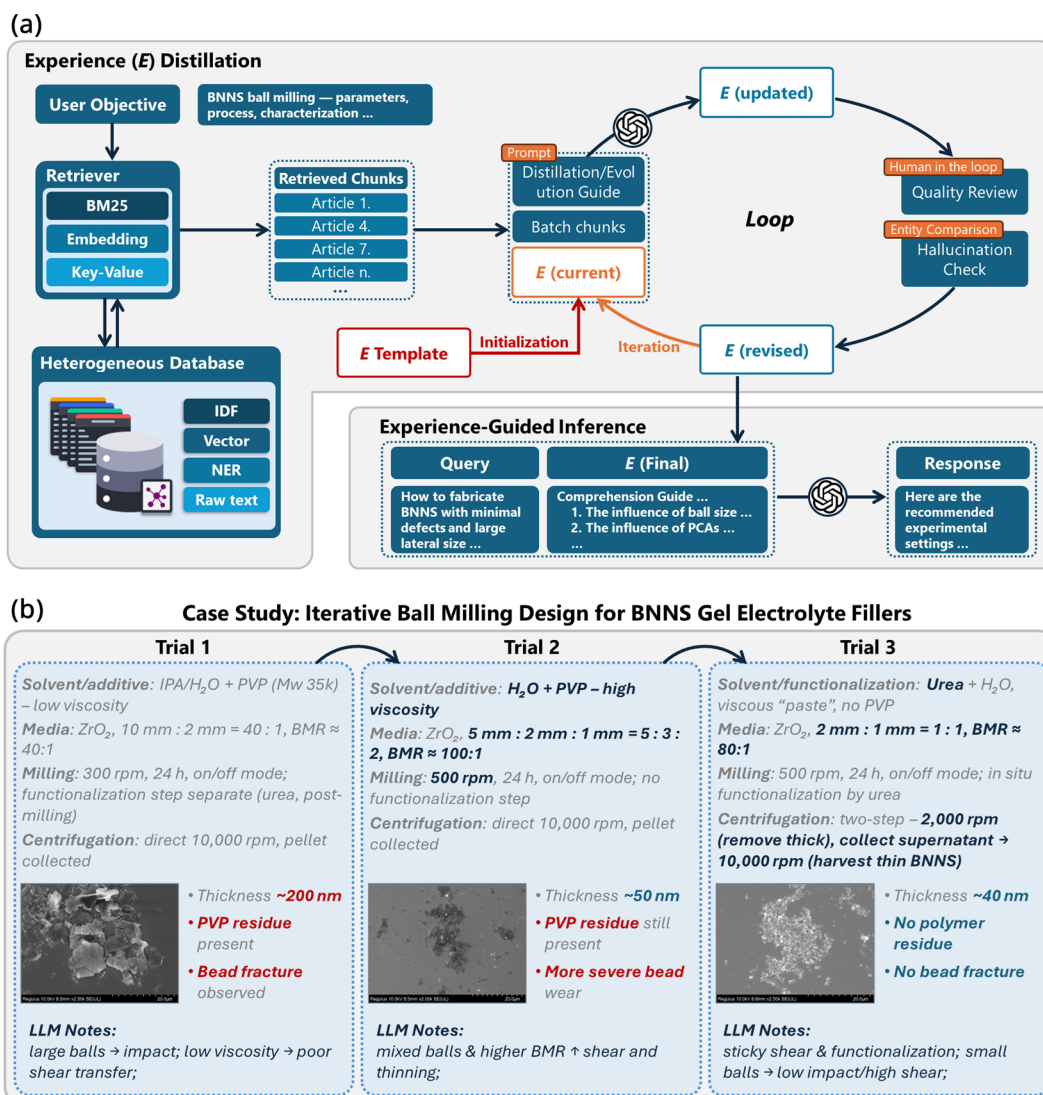


Figure 6: Illustration of the experience-enhanced system based on heterogeneous databases and its application to BNNS ball milling. (a) Schematic of the experience-enhanced system architecture. A user objective is first defined, which guides the retrieval of relevant information from heterogeneous databases. The retrieved results are then processed through an iterative LLM-driven enhancement loop consisting of: 1. experience summarization and integration by the LLM; 2. quality assessment and hallucination analysis; 3. refinement and re-integration of experiences; and 4. iteration back to step 1. or finalization of an enhanced knowledge base, which serves as an experience context for LLM inference. (b) Case study demonstrating how experience-enhanced guidelines were applied to the experimental design of BNNS ball milling for gel electrolyte preparation. The LLM integrated prior knowledge with experimental feedback to iteratively adjust parameters across three cycles, reducing the BNNS thickness from ~ 200 nm to ~ 40 nm while simultaneously eliminating polymer residue and media wear.

improving reproducibility and scalability. More broadly, it illustrates that the system can translate mechanistic priors into actionable process parameters and refine them via

experimental feedback, offering a credible pathway for mechanism-informed, data-efficient optimization in materials processing.

Conclusion and Perspective

This work reconceptualizes materials preparation, BNNS as an example, as a text reasoning task. Rather than searching for fixed numeric optima, we frame synthesis as a decision-making process driven by linguistic logic—conditionality, causality, and trade-offs—embedded in narrative procedures. We leverage large language models (LLMs) as reasoning engines, capable of interpreting complex experimental workflows when provided with appropriate, structured context. To support this, we adopt a context engineering strategy: transforming literature into lightly structured, evidence-linked modules that retain narrative nuance while exposing key entities, parameters, and actions for computation. These modules are organized into a language-native materials database, enabling composite retrieval across semantic, lexical, and explicit constraint axes. This ensures the LLM receives high-quality, task-relevant context to guide reasoning in line with expert deliberation.

In the Experience-Augmented Reasoning (EAR) mode, we further aggregate information across multiple documents to synthesize broader knowledge guides. These guides act as enhanced external context for the LLM—capturing heuristics, typical parameter windows, and failure patterns—which improves the quality and practicality of generated synthesis plans. Combined with Retrieval-Augmented Generation (RAG), this dual-mode framework enables expert-style decisions rooted in both literature evidence and accumulated domain knowledge. Our case study on BNNS–polymer composite preparation demonstrates that this framework enables efficient route planning, failure diagnosis, and parameter tuning under real-world constraints such as material cost, protocol complexity, time, and equipment availability.

Importantly, this text-reasoning framework is complementary and integrable with numerical methods. In scenarios where a single, well-defined preparation route is fixed, conventional numerical machine learning models can still be trained on experimental parameters and outcomes to refine performance prediction. In fact, the theoretical and modeling modules within our language-native database already contain structured descriptions of physical models, equations, and simulation results. These can be retrieved and parsed by the LLM, enabling it to select, apply, or even chain together relevant mathematical models as part of its reasoning process. This allows the system not only to reason with procedural knowledge but also to operate over quantitative, model-based insights, bridging experimental heuristics with theoretical rigor. By integrating symbolic, numerical, and linguistic reasoning, our framework offers a

foundation for hybrid AI agents in materials science—capable of adaptive planning, failure analysis, and performance estimation across both text and number domains.

Finally, we emphasize the broader significance of constructing lightly structured, heterogeneous, language-native databases for scientific domains like materials science. These databases should be structured enough to support retrieval and reasoning, yet flexible enough to preserve the rich procedural logic and narrative cues essential for real-world decision-making. Just as structured numerical datasets have enabled the widespread adoption of machine learning pipelines in materials science, we believe lightly structured text-based datasets—designed for LLM reasoning—represent a complementary paradigm. By preserving narrative context while exposing computable relationships, such datasets serve as an interface between human-readable knowledge and machine-usable logic, and will stand as core infrastructure for future AI-native materials research.

Reference

1. Butler, K.T., Davies, D.W., Cartwright, H. et al. Machine learning for molecular and materials science. *Nature* **559**, 547–555 (2018). <https://doi.org/10.1038/s41586-018-0337-2>
2. Schmidt, J., Marques, M.R.G., Botti, S. et al. Recent advances and applications of machine learning in solid-state materials science. *npj Comput. Mater.* **5**, 83 (2019). <https://doi.org/10.1038/s41524-019-0221-0>
3. Sanchez-Lengeling, B., Aspuru-Guzik, A. Inverse molecular design using machine learning: Generative models for matter engineering. *Science* **361**, 360–365 (2018). <https://doi.org/10.1126/science.aat2663>
4. Himanen, L., Geurts, A., Foster, A.S. et al. Data-Driven Materials Science: Status, Challenges, and Perspectives. *Adv. Sci.* **6**, 1900808 (2019). <https://doi.org/10.1002/advs.201900808>
5. Materials Genome Initiative Strategic Plan. <https://www.mgi.gov>
6. Inorganic Crystal Structure Database (ICSD). <https://icsd.nist.gov>
7. Kearnes, S. M. et al. The Open Reaction Database. *J. Am. Chem. Soc.* **143**, 18820–18826 (2021). <https://doi.org/10.1021/jacs.1c09820>
8. White, A.D. The future of chemistry is language. *Nat. Rev. Chem.* **7**, 457–458 (2023). <https://doi.org/10.1038/s41570-023-00502-0>
9. Olivetti, E. A., Cole, J. M., Kim, E. et al. Data-driven materials research enabled by natural language processing and information extraction. *Appl. Phys. Rev.* **7**, 041304 (2020). <https://doi.org/10.1063/5.0003928>

10. Tshitoyan, V., Dagdelen, J., Weston, L. *et al.* Unsupervised word embeddings capture latent knowledge from materials science literature. *Nature* **571**, 95–98 (2019). <https://doi.org/10.1038/s41586-019-1335-8>
11. Wu, W.; Zheng, M.; Lu, K.; Liu, F.; Song, Y.-H.; Liu, M.; Dang, Z.-M. Thermally Conductive Composites Based on Hexagonal Boron Nitride Nanosheets for Thermal Management: Fundamentals to Applications. *Composites Part A: Applied Science and Manufacturing*. 169 (March), 107533 (2023). <https://doi.org/10.1016/j.compositesa.2023.107533>.
12. Rasul, M.G., Kiziltas, A., Arfaei, B. *et al.* 2D boron nitride nanosheets for polymer composite materials. *npj 2D Mater. Appl.* 5, 56 (2021). <https://doi.org/10.1038/s41699-021-00231-2>
13. Guerra, V., Wan, C., McNally, T. Thermal conductivity of 2D nano-structured boron nitride (BN) and its composites with polymers. *Progress in Materials Science*. 100, 170-186 (2019). <https://doi.org/10.1016/j.pmatsci.2018.10.002>
14. Jablonka, K. M., Ai, Q., Al-Feghali, A. *et al.* 14 examples of how LLMs can transform materials science and chemistry: a reflection on a large language model hackathon. *Digital Discovery* 2, 1233-1250 (2023). <https://doi.org/10.1039/D3DD00113J>
15. Kang, Y., Lee, W., Bae, T. *et al.* Harnessing Large Language Models to Collect and Analyze Metal–Organic Framework Property Data Set. *J. Am. Chem. Soc.* **147**, 3943–3958 (2025). <https://doi.org/10.1021/jacs.4c11085>
16. Schilling-Wilhelmi, M., Ríos-García, M., Shabih, S. *et al.* From text to insight: large language models for chemical data extraction. *Chem. Soc. Rev.* **54**, 1125–1150 (2025). <https://doi.org/10.1039/D4CS00913D>
17. Dagdelen, J., Dunn, A., Lee, S. *et al.* Structured information extraction from scientific text with large language models. *Nat Commun* **15**, 1418 (2024). <https://doi.org/10.1038/s41467-024-45563-x>
18. Zimmermann, Y., Bazgir, A., Al-Feghali, A. *et al.* 34 Examples of LLM Applications in Materials Science and Chemistry: Towards Automation, Assistants, Agents, and Accelerated Scientific Discovery. arXiv:2505.03049 (2025). <https://arxiv.org/abs/2505.03049>
19. Polak, M.P., Morgan, D. Extracting accurate materials data from research papers with conversational language models and prompt engineering. *Nat. Commun.* **15**, 1569 (2024). <https://doi.org/10.1038/s41467-024-45914-8>
20. Zheng, Z., Zhang, O., Borgs, C. *et al.* ChatGPT Chemistry Assistant for Text Mining and the Prediction of MOF Synthesis. *J. Am. Chem. Soc.* **145**, 18048–18062 (2023). <https://doi.org/10.1021/jacs.3c05819>

21. Shetty, P., Rajan, A.C., Kuenneth, C. *et al.* A general-purpose material property data extraction pipeline from large polymer corpora using natural language processing. *npj Comput Mater* **9**, 52 (2023). <https://doi.org/10.1038/s41524-023-01003-w>
22. Swain, M. C., Cole, J. M. ChemDataExtractor: A toolkit for automated extraction of chemical information from the scientific literature. *J. Chem. Inf. Model.* **56**, 1894–1904 (2016). <https://doi.org/10.1021/acs.jcim.6b00207>
23. Skarlinski, M. D., Cox, S., Laurent, J. M. *et al.* Language agents achieve superhuman synthesis of scientific knowledge. *arXiv:2409.13740* (2024). <https://doi.org/10.48550/arXiv.2409.13740>
24. Lála, J., O'Donoghue, O., Shtedritski, A. *et al.* PaperQA: retrieval-augmented generative agent for scientific research. *arXiv: 2312.07559* (2023). <https://doi.org/10.48550/arXiv.2312.07559>
25. Ramos, M. C., Collison, C. J., White, A. D. A review of large language models and autonomous agents in chemistry. *Chem. Sci.* **16**, 2514–2572 (2025). <https://doi.org/10.1039/D4SC03921A>
26. M. Bran, A., Cox, S., Schilter, O. *et al.* Augmenting large language models with chemistry tools. *Nat Mach Intell* **6**, 525–535 (2024). <https://doi.org/10.1038/s42256-024-00832-8>
27. Kang, Y., Kim, J. ChatMOF: an artificial intelligence system for predicting and generating metal-organic frameworks using large language models. *Nat Commun* **15**, 4705 (2024). <https://doi.org/10.1038/s41467-024-48998-4>
28. Szymanski, N.J., Rendy, B., Fei, Y. *et al.* An autonomous laboratory for the accelerated synthesis of novel materials. *Nature* **624**, 86–91 (2023). <https://doi.org/10.1038/s41586-023-06734-w>
29. Yang, Z., Liu, W., Gao, B. *et al.* MOOSE-Chem: Large language models for rediscovering unseen chemistry scientific hypotheses. *arXiv* (2025). <https://arxiv.org/abs/2410.07076>
30. Zhang, H., Song, Y., Hou, Z. *et al.* HoneyComb: A flexible LLM-based agent system for materials science. *arXiv* (2024). <https://arxiv.org/abs/2409.00135>
31. Zheng, Z., Rampal, N., Inizan, T.J. *et al.* Large language models for reticular chemistry. *Nat Rev Mater* **10**, 369–381 (2025). <https://doi.org/10.1038/s41578-025-00772-8>
32. Ferber, D., El Nahhas, O.S.M., Wölflein, G. *et al.* Development and validation of an autonomous artificial intelligence agent for clinical decision-making in oncology. *Nat Cancer* **6**, 1337–1349 (2025). <https://doi.org/10.1038/s43018-025-00991-6>

33. Hippalgaonkar, K., Li, Q., Wang, X. *et al.* Knowledge-integrated machine learning for materials: lessons from gaming and robotics. *Nat Rev Mater* **8**, 241–260 (2023). <https://doi.org/10.1038/s41578-022-00513-1>
34. Boiko, D. A.; MacKnight, R.; Kline, B.; Gomes, G. Autonomous Chemical Research with Large Language Models. *Nature* **624**, 570–578 (2023) <https://doi.org/10.1038/s41586-023-06792-0>
35. Jablonka, K.M., Schwaller, P., Ortega-Guerrero, A. *et al.* Leveraging large language models for predictive chemistry. *Nat Mach Intell* **6**, 161–169 (2024). <https://doi.org/10.1038/s42256-023-00788-1>
36. Ye, Y., Ren, J., Wang, S. *et al.* Construction and Application of Materials Knowledge Graph in Multidisciplinary Materials Science via Large Language Model. In *Advances in Neural Information Processing Systems* **37**, 56878–56897 (2024). <https://bytez.com/docs/neurips/95920/paper>
37. McCusker, J. P., Keshan, N., Rashid, S., Deagen, M., Brinson, C. & McGuinness, D. L. NanoMine: A Knowledge Graph for Nanocomposite Materials Science. In *The Semantic Web – ISWC 2020* (eds Pan, J. Z., Tamma, V., d’Amato, C., Janowicz, K., Fu, B., Polleres, A., Seneviratne, O. & Kagal, L.) Vol. 12507, 144–159 (Springer International Publishing, 2020). https://doi.org/10.1007/978-3-030-62466-8_10
38. Venugopal, V., Olivetti, E. MatKG: An autonomously generated knowledge graph in Material Science. *Sci Data* **11**, 217 (2024). <https://doi.org/10.1038/s41597-024-03039-z>
39. Nie, Z., Zheng, S., Liu, Y. *et al.* Automating materials exploration with a semantic knowledge graph for Li-ion battery cathodes. *Adv. Funct. Mater.* **32**, 2201437 (2022). <https://doi.org/10.1002/adfm.202201437>
40. Garay-Ruiz, D., Bo, C. Chemical reaction network knowledge graphs: the OntoRXN ontology. *J Cheminform* **14**, 29 (2022). <https://doi.org/10.1186/s13321-022-00610-x>
41. Rydholm, E., Bastys, T., Svensson, E. *et al.* Expanding the chemical space using a chemical reaction knowledge graph. *Digital Discovery* **3**, 1378–1388 (2024). <https://doi.org/10.1039/D3DD00230F>
42. Statt, M. J., Rohr, B. A., Guevarra, D. *et al.* The materials experiment knowledge graph. *Digital Discovery* **2**, 909–914 (2023). <https://doi.org/10.1039/D3DD00067B>
43. Yuan, Y., Liu, C., Yuan, J. *et al.* A hybrid RAG system with comprehensive enhancement on complex reasoning. *arXiv*: 2408.05141 (2024). <https://arxiv.org/abs/2408.05141>

44. Han, H., Wang, Y., Shomer, H. et al. Retrieval-augmented generation with graphs (GraphRAG). *arXiv*: 2501.00309 (2025). <https://arxiv.org/abs/2501.00309>
45. Lewis, P., Perez, E., Piktus, A. et al. Retrieval-augmented generation for knowledge-intensive NLP tasks. In *Advances in Neural Information Processing Systems* (eds. H. Larochelle et al.) (NeurIPS, 2020). <https://doi.org/10.5555/3495724.3496517>
46. Liu, N. F., Lin, K., Hewitt, J. et al. Lost in the middle: how language models use long contexts. *arXiv*:2307.03172 (2023). <https://doi.org/10.48550/arXiv.2307.03172>
47. Gao, Y., Xiong, Y., Gao, X. et al. Retrieval-Augmented Generation for Large Language Models: A Survey. *arXiv*:2312.10997 (2024). <https://doi.org/10.48550/arXiv.2312.10997>
48. Zhong, X., Jin, B., Ouyang, S. et al. Benchmarking retrieval-augmented generation for chemistry. *arXiv*: 2505.07671 (2025). <https://arxiv.org/abs/2505.07671>
49. Ayala, O., Bechard, P. Reducing hallucination in structured outputs via Retrieval-Augmented Generation. In *Proceedings of the 2024 Conference of the North American Chapter of the Association for Computational Linguistics: Human Language Technologies (Volume 6: Industry Track)* (eds. Yang, Y., Davani, A., Sil, A. & Kumar, A.) 228–238 (Association for Computational Linguistics, 2024). <https://doi.org/10.18653/v1/2024.naacl-industry.19>
50. Glass, M., Rossiello, G., Chowdhury, M. F. M. et al. Re2G: Retrieve, rerank, generate. In *Proceedings of the 2022 Conference of the North American Chapter of the Association for Computational Linguistics: Human Language Technologies* (eds. Carpuat, M., de Marneffe, M.-C. & Meza Ruiz, I. V.) 2701–2715 (Association for Computational Linguistics, 2022). <https://doi.org/10.18653/v1/2022.naacl-main.194>
51. Wellawatte, G. P., Guo, H., Lederbauer, M. et al. ChemLit-QA: a human evaluated dataset for chemistry RAG tasks. *Mach. Learn.: Sci. Technol.* **6**, 020601 (2025). <https://doi.org/10.1088/2632-2153/acxyz1>
52. Leng, Y., Zhong, Y., Gu, Z. et al. Intelligent, personalized scientific assistant via large language models for solid-state battery research. *ACS Materials Lett.* **7**, 1807–1816 (2025). <https://doi.org/10.1021/acsmaterialslett.4c02674>
53. Prince, M.H., Chan, H., Vriza, A. et al. Opportunities for retrieval and tool augmented large language models in scientific facilities. *npj Comput Mater* **10**, 251 (2024). <https://doi.org/10.1038/s41524-024-01423-2>
54. Tang, Y., Xu, W., Cao, J. et al. MatterChat: A multi-modal LLM for material science. *arXiv*: 2502.13107 (2025). <https://arxiv.org/abs/2502.13107>

55. Ghafarollahi, A. & Buehler, M. J. AtomAgents: Alloy design and discovery through physics-aware multi-modal multi-agent artificial intelligence. *arXiv*: 2407.10022 (2024). <https://arxiv.org/abs/2407.10022>
56. Zhao, Z., Chen, B., Li, J. et al. ChemDFM-X: towards large multimodal model for chemistry. *Sci. China Inf. Sci.* **67**, 220109 (2024). <https://doi.org/10.1007/s11432-024-4243-0>
57. Stewart, I., Buehler, M. J. Molecular analysis and design using generative artificial intelligence via multi-agent modeling. *Mol. Syst. Des. Eng.* **10**, 314–337 (2025). <https://doi.org/10.1039/D4ME00174E>